The Certicom Challenges ECC2-X

Daniel V. Bailey[1], Brian Baldwin[2], Lejla Batina[3], Daniel J. Bernstein[4], Peter Birkner[5], Joppe W. Bos[6], Gauthier van Damme[3], Giacomo de Meulenaer[7], Junfeng Fan[3], Tim Güneysu[8], Frank Gurkaynak[9], Thorsten Kleinjung[6], Tanja Lange[5], Nele Mentens[3], Christof Paar[8], Francesco Regazzoni[7], Peter Schwabe[5], and Leif Uhsadel[3] [*]

[1] RSA, the Security Division of EMC, USA
dbailey@rsa.com
[2] Claude Shannon Institute for Discrete Mathematics, Coding and Cryptography.
Dept. of Electrical & Electronic Engineering, University College Cork, Ireland
brianb@rennes.ucc.ie
[3] ESAT/SCD-COSIC, Katholieke Universiteit Leuven and IBBT
Kasteelpark Arenberg 10, B-3001 Leuven-Heverlee, Belgium
[4] Department of Computer Science
University of Illinois at Chicago, Chicago, IL 60607–7045, USA
djb@cr.yp.to
[5] Department of Mathematics and Computer Science
Technische Universiteit Eindhoven, P.O. Box 513, 5600 MB Eindhoven, Netherlands
p.birkner@tue.nl, tanja@hyperelliptic.org, peter@cryptojedi.org
[6] EPFL IC IIF LACAL, Station 14, CH-1015 Lausanne, Switzerland
{joppe.bos, thorsten.kleinjung}@epfl.ch
[7] UCL Crypto Group, Place du Levant, 3, B-1348 Louvain-la-Neuve, Belgium
{giacomo.demeulenaer, francesco.regazzoni}@uclouvain.be
[8] Horst Görtz Institute for IT Security, Ruhr University Bochum, Germany
{gueneysu, cpaar}@crypto.rub.de
[9] Microelectronics Design Center, ETH Zürich, Switzerland
kgf@ee.ethz.ch

Abstract. To encourage research on the hardness of the elliptic-curve discrete-logarithm problem (ECDLP) Certicom has published a series of challenge curves and DLPs.

This paper analyzes the costs of breaking the Certicom challenges over the binary fields $\mathbf{F}_{2^{131}}$ and $\mathbf{F}_{2^{163}}$ on a variety of platforms. We describe details of the choice of step function and distinguished points for the Koblitz and non-Koblitz curves. In contrast to the implementations for the previous Certicom challenges we do not restrict ourselves to software and conventional PCs, but branch out to cover the majority of available platforms such as various ASICs, FPGAs, CPUs and the Cell Broadband Engine. For the field arithmetic we investigate polynomial and normal basis arithmetic for these specific fields; in particular for the challenges on Koblitz curves normal bases become more attractive on ASICs and

FPGAs.

Keywords: ECC, binary fields, Certicom challenges

1   Introduction

In 1997, Certicom published several challenges [Cer97a] to solve the Discrete Logarithm Problem (DLP) on elliptic curves. The challenges cover curves over prime fields and binary fields at several different sizes. For the binary curves, each field size has two challenges: a Koblitz curve and a random curve defined over the full field.

For small bit sizes the challenges were broken quickly — the 79-bit challenges fell already in 1997, those with 89 bits in 1998 and those with 97 bits in 1998 and 1999; Certicom described these parameter sizes as training exercises. In April 2000, the first Level I challenge (the Koblitz curve ECC2K-108) was solved by Harley's team in a distributed effort [Har] on a multitude of PCs on the Internet. After that, it took some time until the remaining challenges with 109 bit fields were tackled. The ECCp-109 (elliptic curve over a prime field of 109 bits) was solved on November 2002 and the ECC2-109 (random elliptic curve over a binary field with 109 bits) was solved in April 2004; both efforts were organized by Chris Monico. The gap of more than one year between the results is mostly due to the Koblitz curves offering less security per bit than curves defined over the extension field or over prime fields. The Frobenius endomorphism can be used to speed up the protocols using elliptic curves — the main reason Koblitz curves are attractive in practice — but it also gives an advantage to the attacker. In particular, over $\mathbf{F}_{2^n}$ the attack is sped up by a factor of approximately $\sqrt{n}$.

Since 2004 not much was heard about attempts to break the larger challenges. Certicom's documentation states "The 109-bit Level I challenges are feasible using a very large network of computers. The 131-bit Level I challenges are expected to be infeasible against realistic software and hardware attacks, unless of course, a new algorithm for the ECDLP is discovered. The Level II challenges are infeasible given today's computer technology and knowledge."

In this paper we analyze the cost of breaking the binary Certicom challenges: ECC2K-130, ECC2-131, ECC2K-163 and ECC2-163. We collect timings for field arithmetic in polynomial and normal basis representation for several different platforms which the authors of this paper have at their disposal and outline the ways of computing discrete logarithms on these curves. For Koblitz curves, the Frobenius endomorphism can be used to speed up the attack by working with classes of points. The step function in Pollard's rho method has to be adjusted to deal with classes. Per step a few more squarings are needed but the overall savings in the number of steps is quite dramatic.

The SHARCS community has already had some analysis of the costs of breaking binary ECC on FPGAs at SHARCS'06 [BMdDQ06]. Our analysis is an update of those results for current FPGAs and covers the concrete challenges. Particular emphasis is placed on the FPGA used in the Copacobana FPGA cluster. This way, part of the attack can be run on this cluster. Our research goes

further than [BMdDQ06] by dealing with other curves, considering many other platforms and analyzing the best methods for how these platforms can work together on computing discrete logarithms.

Our main conclusion is that the "infeasible" ECC2K-130 challenge is in fact feasible. For example, our implementations can break ECC2K-130 in an expected time of a year using only 4200 Cell processors, or using only 220 ASICs. For comparison, [BMdDQ06] and [MdDBQ07] estimated a cost of nearly \$20000000 to break ECC2K-130 in a year.

As validation of the designs and the performance estimates we reimplemented and reran the ECC2K-95 challenge, using 30 2.4GHz cores on a Core 2 cluster for a few days to re-break the ECC2K-95 challenge. Each core performed 4.7 million iterations per second and produced distinguished points at the predicted speed. For comparison, Harley's original ECC2K-95 solution took 25 days on 200 Alpha workstations, the fastest being 0.6GHz cores performing 0.177 million iterations per second. The improvement is due not only to increased processor speeds but also to improved implementation techniques described in this paper.

The project partners are working on collecting enough hardware to actually carry out the ECC2K-130 attack. Available resources include KU Leuven's VIC cluster (`https://vscentrum.be/vsc-help-center/reference-manuals/vic-user-manual` and `vic3-user-manual`); several smaller clusters such as TU Eindhoven's CCCC cluster (`http://www.win.tue.nl/cccc/`); several high-end GPUs (not yet covered in this paper); some FPGA clusters; and possibly some ASICs. This is the first time that one of the Certicom challenges is tackled with a broad mix of platforms. This set-up requires extra considerations for the choice of the step function and the distinguished points so that all platforms can cooperate in finding collisions despite different preferences in point representation.

2 The Certicom challenges

Each challenge is to compute the ECC private key from a given ECC public key, i.e. to solve the discrete-logarithm problem in the group of points of an elliptic curve over a field $\mathbf{F}_{2^n}$. The complete list of curves is published online at [Cer97b]. In the present paper, we tackle the curves ECC2K-130, ECC2-131, ECC2K-163, and ECC2-163, the parameters of which are given below.

The parameters are to be interpreted as follows: The curve is defined over the finite field represented by $\mathbf{F}_2[z]/F(z)$, where $F(z)$ is the monic irreducible polynomial of degree n given below for each challenge. Field elements are given as hexadecimal numbers which are interpreted as bit strings giving the coefficients of polynomials over $\mathbf{F}_2$ of degree less than n. The curves are of the form $y^2 + xy = x^3 + ax^2 + b$, with $a, b \in \mathbf{F}_{2^n}$. For the Koblitz curve challenges the curves are defined over $\mathbf{F}_2$, i.e. $a, b \in \mathbf{F}_2$. The points P and Q are given by their coordinates $P = (\texttt{P\_x}, \texttt{P\_y})$ and $Q = (\texttt{Q\_x}, \texttt{Q\_y})$. The group order is $h \cdot \ell$, where ℓ is a prime and h is the cofactor.

– ECC2K-130 ($F = z^{131} + z^{13} + z^2 + z + 1$)

```
a = 0, b = 1
P_x = 05 1C99BFA6 F18DE467 C80C23B9 8C7994AA
P_y = 04 2EA2D112 ECEC71FC F7E000D7 EFC978BD
h = 04, l = 2 00000000 00000000 4D4FDD57 03A3F269
Q_x = 06 C997F3E7 F2C66A4A 5D2FDA13 756A37B1
Q_y = 04 A38D1182 9D32D347 BD0C0F58 4D546E9A
```

– ECC2-131 ($F = z^{131} + z^{13} + z^2 + z + 1$)

```
a = 07 EBCB7EEC C296A1C4 A1A14F2C 9E44352E
b = 00 610B0A57 C73649AD 0093BDD6 22A61D81
P_x = 00 439CBC8D C73AA981 030D5BC5 7B331663
P_y = 01 4904C07D 4F25A16C 2DE036D6 0B762BD4
h = 02, l = 04 00000000 00000002 6ABB991F E311FE83
Q_x = 06 02339C5D B0E9C694 AC890852 8C51C440
Q_y = 04 F7B99169 FA1A0F27 37813742 B1588CB8
```

– ECC2K-163 ($F = z^{163} + z^8 + z^2 + z + 1$)

```
a = 1, b = 1
P_x = 02 091945E4 2080CD9C BCF14A71 07D8BC55 CDD65EA9
P_y = 06 33156938 33774294 A39CF6F8 C175D02B 8E6A5587
h = 02, l = 04 00000000 00000000 00020108 A2E0CC0D 99F8A5EF
Q_x = 00 7530EE86 4EDCF4A3 1C85AA17 C197FFF5 CAFECAE1
Q_y = 07 5DB1E80D 7C4A92C7 BBB79EAE 3EC545F8 A31CFA6B
```

– ECC2-163 ($F = z^{163} + z^8 + z^2 + z + 1$)

```
a = 02 5C4BEAC8 074B8C2D 9DF63AF9 1263EB82 29B3C967
b = 00 C9517D06 D5240D3C FF38C74B 20B6CD4D 6F9DD4D9
P_x = 02 3A2E9990 4996E867 9B50FF1E 49ADD8BD 2388F387
P_y = 05 FCBFE409 8477C9D1 87EA1CF6 15C7E915 29E73BA2
h = 02, l = 04 00000000 00000000 0001E60F C8821CC7 4DAEAFC1
Q_x = 04 38D8B382 1C8E9264 637F2FC7 4F8007B2 1210F0F2
Q_y = 07 3FCEA8D5 E247CE36 7368F006 EBD5B32F DF4286D2
```

The curves denoted ECC2K-X are binary Koblitz curves. This means that their equation is defined over $\mathbf{F}_2$ which, in turn, implies that the Frobenius endomorphism σ operates on the set of points over $\mathbf{F}_{2^n}$. Because σ commutes with scalar multiplication, it operates on prime-order subgroups as a group automorphism. Consequently, there exists an integer s which is unique modulo ℓ so that $\sigma(P) = [s]P$ for all points P in the subgroup of order ℓ. The value of s is computed as $T - s = \gcd(T^n - 1, T^2 + (-1)^a T + 2)$ in $\mathbf{F}_\ell[T]$.

3 Parallelized Pollard's rho algorithm

In this section, we explain the parallelized version of Pollard's rho method. First, we describe the single-instance version of the method and then show how to parallelize it with the distinguished-point method as done by van Oorschot and Wiener in [vOW99]. Note that these descriptions give the "school-book versions" for background; details on our actual implementation are given in Section 6.

3.1 Single-instance Pollard rho

Pollard's rho method is an algorithm to compute the discrete logarithm in generic cyclic groups. It was originally designed for finding discrete logarithms in $\mathbf{F}_p^*$ [Pol78] and is based on Floyd's cycle-finding algorithm and the birthday paradox. In the following, let G be a cyclic group, using additive notation, of order ℓ with a generator P. Given $Q \in G$, our goal is to find an integer k such that $[k]P = Q$.

The idea of Pollard's rho method is to construct a sequence of group elements with the help of an iteration function $f : G \to G$. This function generates a sequence

$$P_{i+1} = f(P_i),$$

for $i \geq 0$ and some initial point P_0. We compute elements of this sequence until a collision of two elements occurs. A collision is an equality $P_q = P_m$ with $q \neq m$. Let us assume we know how to write the elements P_i of the sequence as $P_i = [a_i]P \oplus [b_i]Q$, then we can compute the discrete logarithm $k = \log_P(Q) = \frac{a_q - a_m}{b_m - b_q}$ if a collision $P_q = P_m$ with $b_m \neq b_q$ has occurred. We show later how to obtain such sequences.

Assuming the iteration function is a random mapping of size ℓ, i.e. f is equally probable among all functions $G \to G$, Harris in [Har60] showed that the expected number of steps before a collision occurs is approximately $\sqrt{\pi\ell/2}$. The sequence $(P_i)_{i \geq 0}$ is called a *random walk* in G.

A pictorial description of the rho method can be given by drawing the Greek letter ρ representing the random walk and starting at the tail at P_0. "Walking" along the line means going from P_i to P_{i+1}. If a collision occurs at P_t, then $P_t = P_{t+s}$ for some integer s, and the elements $P_t, P_{t+1}, \ldots, P_{t+s-1}$ form a loop. See Figure 1, and see Figure 2 for an example of how this picture occurs inside the complete graph of a function.

In the original paper by Pollard it is proposed to find a collision with Floyd's cycle-finding algorithm. The idea of this algorithm is to walk along the sequence at two different speeds and wait for a collision. This is usually realized by using the two sequences P_i and P_{2i}. Doing a step means to increase i by 1. If $P_i = P_{2i}$ for some i, then we have found a collision.

To benefit from this method it is necessary to construct walks on G that behave like random mappings and for which for each element a representation as $P_i = [a_i]P \oplus [b_i]Q$ is known. An example of a such a class of walks is the r-adding walk as studied by Teske [Tes01]. The group G is divided in r partitions using a partition function $\psi : G \to [0, r-1]$. An element $R_j = [c_j]P \oplus [d_j]Q$, for
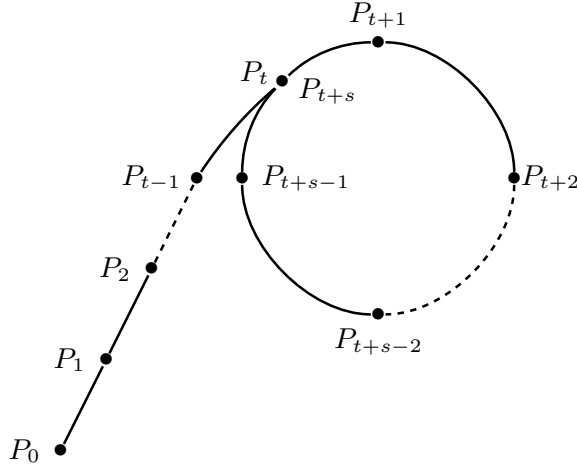
Fig. 1. Abstract diagram of the rho method.

random c_j and d_j, is associated to each partition and the iteration function is defined as

$$P_{i+1} = f(P_i) = P_i \oplus R_{\psi(P_i)},$$

and the values of a_i and b_i are updated as $a_{i+1} = a_i + c_j, \ b_{i+1} = b_i + d_j$. When a collision $P_q = P_m$ for $q \neq m$ is found, then we obtain

$$[a_q]P \oplus [b_q]Q = [a_m]P \oplus [b_m]Q,$$

which implies $(a_q - a_m)P = (b_m - b_q)Q$ and hence $k = \log_P(Q) = \frac{a_q - a_m}{b_m - b_q}$. This solves the discrete-logarithm problem. With negligible probability the difference $b_m - b_q = 0$; in this case the computation has to be restarted with a different starting point P_0. Teske showed that choosing $r = 20$ and random values for the c_j and d_j approximates a random walk sufficiently well for the purpose of analyzing the function. For implementations, a power of 2 such as $r = 8$ or $r = 16$ or $r = 32$ is more practical.

3.2   Parallelized version and distinguished points

When running N instances of Pollard's rho method concurrently, a speed-up of $\sqrt{N}$ is obtained. To get a linear speedup, i.e. by a factor N, and thus to parallelize Pollard's rho method efficiently, van Oorschot and Wiener [vOW99] proposed the distinguished-points method. It works as follows: One defines a subset D of G such that D consists of all elements that satisfy a particular condition. For example, we can choose D to contain all group elements whose s least significant bits are zero, for some positive integer s. This allows to easily check if a group element is in D or not.
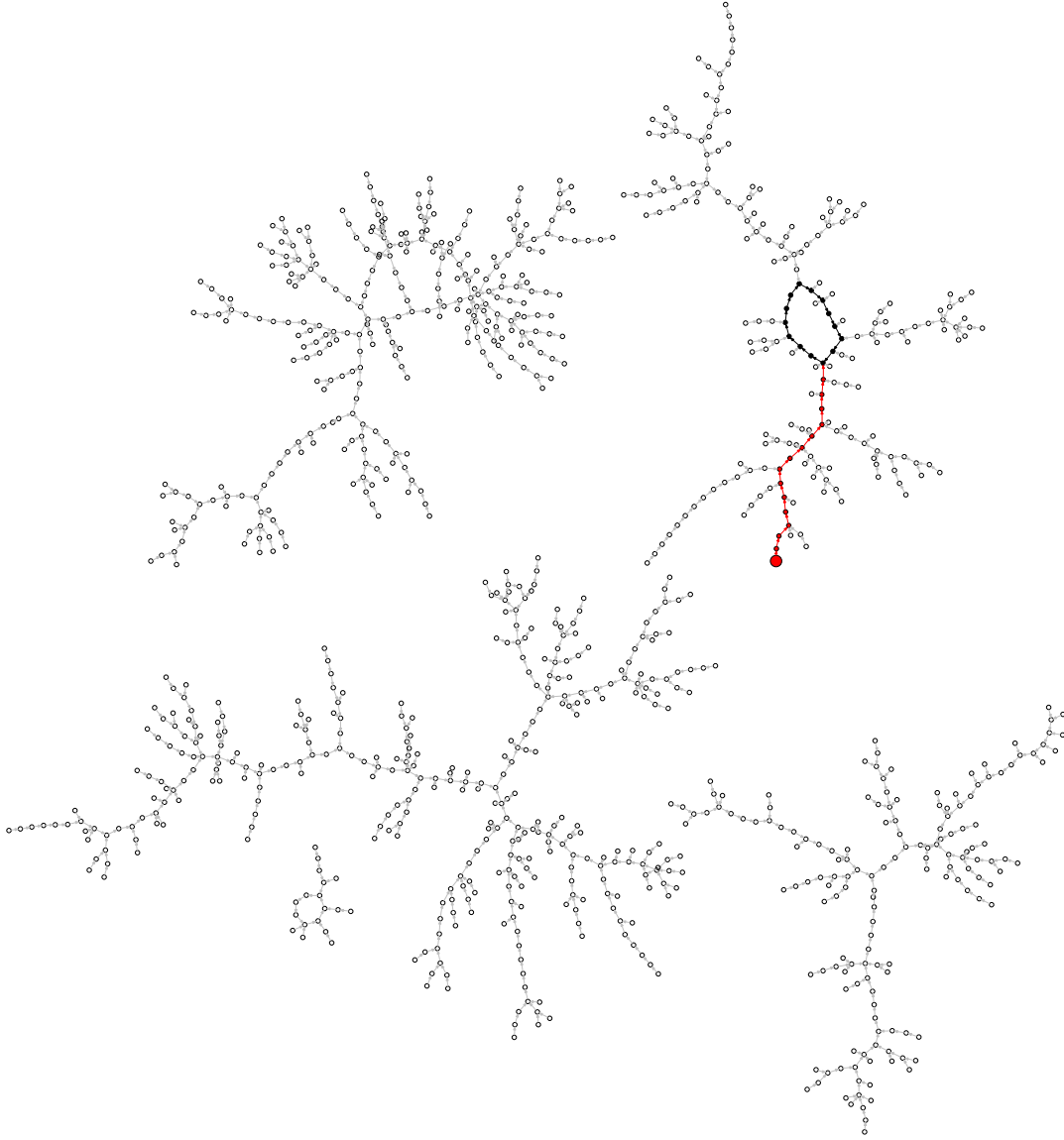
Fig. 2. Example of the rho method. There are 1024 circles representing elements of a set of size 1024. Each circle has an arrow to a randomly chosen element of the set; the positions of circles in the plane are chosen (by the `neato` program) so that these arrows are short. A walk begins at a random point indicated by a large red circle. The walk stops when it begins to cycle; the cycle is shown in black. This walk involves 29 elements of the set.
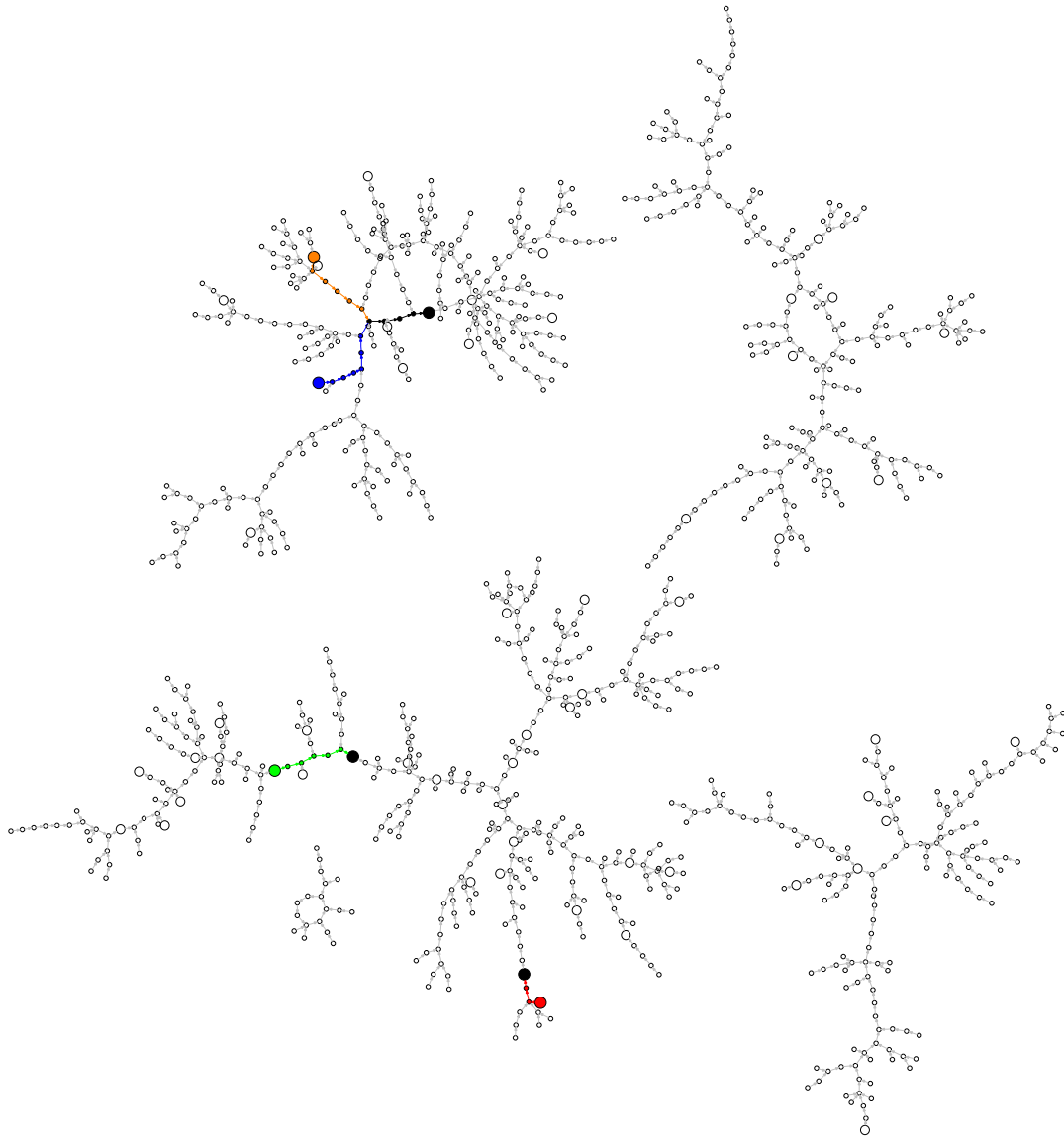
Fig. 3. Example of the parallelized rho method. Arrows represent the same randomly generated function used in Figure 2. Each circle is, with probability 1/16, designated a distinguished point and drawn as a large hollow circle. Four walks begin at random points indicated by large red, green, blue, and orange circles. Each walk stops when it reaches a distinguished point; those distinguished points are shown in black. The blue and orange walks collide and find the same distinguished point.

Each instance starts at a new linear combination $[a_0]P \oplus [b_0]Q$ and performs the random walk until a distinguished point is found. The distinguished point, together with the coefficients a_i, b_i that lead to it, is then stored on a central server. The server checks for collisions within the set of distinguished points and can solve the DLP once one collision is found. As before, the difference $b_m - b_q$ can be zero. In this case the distinguished point P_q is discarded and the search continues; note that the other stored distinguished points can lead to collisions since all processes are started independently at random.

See Figure 3 for an illustration of the distinguished-points method.

4 Automorphisms of small order

Elliptic-curve groups allow very fast negation. On binary curves such as the Certicom challenge curves, the negative of $P = (x, y)$ is $-P = (x, y + x)$. One can speed up the rho method by a factor of $\sqrt{2}$ (cf. [WZ98]) by choosing an iteration function defined on sets $\{P, -P\}$. For example, one can take any iteration function g, and define $f(x, y)$ as $g(\min\{(x, y), (x, y + x)\})$, ensuring that $f(-P) = f(P)$. Here min means lexicographic minimum. Special care has to be taken to avoid fruitless short cycles; see method 1 below for details.

The ECC2-131 challenge has group size $n \approx 2^{130}$; up to negation there are $n/2 \approx 2^{129}$ sets $\{P, -P\}$. In this case the expected number of steps is approximately $\sqrt{\pi n/4} \approx 2^{64.8}$. The ECC2-163 challenge has group size $n \approx 2^{162}$; in this case $\sqrt{\pi n/4} \approx 2^{80.8}$.

The ECC2K-130 challenge has group size $n \approx 2^{129}$. The DLP is easier than for the ECC2-131 challenge because this curve is a Koblitz curve allowing a very fast Frobenius endomorphism. Specifically, if (x, y) is on the ECC2K-130 curve then $\sigma(x, y) = (x^2, y^2), \sigma^4(x, y) = (x^4, y^4)$ and so on through $(x^{2^{130}}, y^{2^{130}})$ are on the ECC2K-130 curve; note that $(x^{2^{131}}, y^{2^{131}}) = (x, y)$. One can speed up the rho method by an additional factor of $\sqrt{131}$ by choosing an iteration function defined on sets $\{\pm\sigma^i(x, y) | 0 \leq i < n\}$; there are only about $n/262 \approx 2^{121}$ of these sets. In this case the expected number of rho iterations is approximately $\sqrt{\pi n/524} \approx 2^{60.8}$. Similarly, the expected number of iterations for the ECC2K-163 challenge is approximately $2^{77.2}$.

The remainder of this section focuses on Koblitz curves, i.e. curves defined over $\mathbf{F}_2$ that are considered over extension fields $\mathbf{F}_{2^n}$ and considers how to define walks on classes under the Frobenius endomorphism.

Speedups for solving the DLP on elliptic curves with automorphisms were studied by several groups independently. The following text summarizes the contributions by Wiener and Zuccherato [WZ98], Gallant, Lambert, and Vanstone [GLV00], and Harley [Har]. In the following we describe two methods to define a (pseudo-)random walk on the classes of points, where the class of a point P also contains $-P, \pm\sigma(P), \pm\sigma^2(P), \ldots, \pm\sigma^{n-1}(P)$.

4.1   Method 1

This method was discovered by Wiener and Zuccherato [WZ98] and Gallant, Lambert, and Vanstone [GLV00]. To apply the parallel Pollard rho method, the iteration function (or step function) in the first method uses a r-adding walk (see [Tes01]), i.e. we have r pre-defined random points $R_0, \ldots, R_{r-1}$ on the curve. To perform a step of the walk, we add one of the R_j's to the current point P_i to obtain P_{i+1}. To determine which point to add to P_i, we partition the group of points on the curve into r sets and define the map

$$\psi : E(\mathbf{F}_{2^n}) \mapsto \{0, \ldots, r-1\}, \tag{1}$$

which assigns to each point on the curve one of the r partitions. With this map, we could define the walk and the iteration function f as follows:

$$P_{i+1} = f(P_i) = P_i \oplus R_{\psi(P_i)}. \tag{2}$$

However, more care is required to avoid fruitless, short cycles. Assume that P_i is such that the unique representative of the class of $P_{i+1} = P_i \oplus R_{\psi(P_i)}$ is $-P_{i+1}$; this happens with probability $1/(2n)$. With probability $1/r$ the next added point $R_{\psi(-P_{i+1})}$ equals $R_{\psi(P_i)}$ and thus $P_{i+2} = P_i$ and the walk will never leave this cycle. The probability of such cycles is $1/(2rn)$ and is thereby rather high. See [WZ98] for a method to detect and deal with such cycles.

   We define the unique representative per class by lexicographically ordering all x-coordinates of the points in the class and choosing the "smallest" element in that order. This element has most zeros starting from the most significant bit. Of the two possible y-coordinates chose the one with lexicographically smaller value. Given that y and $y + x$ are the candidate values and that the number of leading zeros of x is known already, say i, it is easy to grab the distinguishing bit in the y-coordinate as the $(i+1)$-th bit starting from the most significant bit. Let $\Phi(P)$ be this unique representative of the class containing P and let $(b_4, b_3, b_2, b_1, 1)$ be the five least significant bits of $\Phi(P)$. Let $j = (b_4, b_3, b_2, b_1)_2$. Then we can define the value of $\psi(P)$ to be $j \in \{0, \ldots, 15\}$. The iteration function is then given by

$$P_{i+1} = f(P_i) = \Phi(P_i) \oplus R_{\psi(P_i)}.$$

   To parallelize Pollard rho, we also need to define distinguished points (or rather distinguished classes in the present case). For each class, we use the m most significant bits of $x(\Phi(P))$. If these bits are all zero, then we define this point (class) to be a distinguished one. With this, we can apply the methods from Section 3.

4.2   Method 2

A method similar to the second method was described by Gallant, Lambert, and Vanstone [GLV00]; Harley [Har] uses a similar method in his code to attack the earlier Certicom challenges.

This method does not need any precomputed random points R_i on the curve. Instead, we define the walk and the iteration function f as

$$P_{i+1} = f(P_i) = P_i \oplus \sigma^j(P_i), \tag{3}$$

where j is the Hamming weight of the binary representation of $x(P_i)$ in normal basis representation and σ the Frobenius automorphism. Note that if the computations are not carried out in normal-basis representation it is necessary to change the representation of $x(P)$ from polynomial basis to normal basis at every step. Note that in normal-basis representation the Hamming weight of $x(P_i)$ is equal to the Hamming weight of $x(\pm\sigma^k(P_i))$ for all $k \in \{0, \dots, 130\}$. Note also that

$$\pm\sigma(P_{i+1}) = \pm\sigma(P_i) \pm \sigma^j(\sigma(P)) = f(\pm\sigma(P))$$

and thus the step function is well defined on the classes.

For parallel Pollard rho, we also need to define distinguished points (classes). For example, we can say that a class is a distinguished one if the Hamming weight of $x(P)$ is less than or equal to w for some fixed value of w. Note that the value of a determines the parity of the Hamming weight since for all points $\text{Tr}(x(P)) = \text{Tr}(a)$. This means that $(\binom{n}{w} + \binom{n}{w-2} + \cdots)/2^{n-1}$ approximates the probability of distinguished points as only about 2^{n-1} different values can occur as x-coordinates.

The proposed version by Gallant, Lambert, and Vanstone [GLV00] does not use the Hamming weight to define j. Instead they use a unique representative per class, e.g. the point with lexicographically smallest x-coordinate, and put $j = \text{hash}(x(P))$ for hash a hash function from $\mathbf{F}_{2^n}$ to $\{0, 1, \dots, n-1\}$. Using the Hamming weight of $x(P)$ instead avoids the computation of the unique representative at the expense of a somewhat less random walk. There are many more points with a Hamming weight around $n/2$ than there are around the extremal values 0 and $n-1$. See Section 6.2 for analysis of the loss of randomness.

Harley included an extra tweak to method 2 by using the Hamming weight for updating the points but restricting the maximal exponent of σ in

$$P_{i+1} = f(P_i) = P_i \oplus \sigma^{\bar{j}}(P_i), \tag{4}$$

by taking $\bar{j}$ as essentially the remainder of j modulo 7. He observed that for $n = 109$ the equality $(1 + \sigma^3) = -(1 + \sigma)$ holds. He settled for scalars $(1 + \sigma^1), (1 + \sigma^2), (1 + \sigma^4), (1 + \sigma^5), (1 + \sigma^6), (1 + \sigma^7)$, and $(1 + \sigma^8)$. This limits the number of times σ has to be applied per step. For sizes larger than 109 somewhat larger exponents should be used. The walks resulting from this method are even less resembling random walks but the computation is sped up by requiring fewer squarings.

5   Cost estimates

In this section we apply Pollard's rho method to elliptic curves and give rough cost estimates in terms of field operations. The next sections will translate these

estimates to the different computation platforms we use in our attack. The fine tuning for the Certicom challenge ECC2K-130 is given in Section 6. In the following we use $\mathbf{I}$ to denote the cost of a field inversion, $\mathbf{M}$ to denote the cost of a field multiplication, and $\mathbf{S}$ to denote the cost of a field squaring.

5.1   Point representation and addition

Most high-speed implementations of elliptic-curve cryptography use inversion-free coordinate systems for the scalar multiplication, i.e. they use a redundant representation $P = (X_P : Y_P : Z_P)$ to denote the affine point $(X_P/Z_P, Y_P/Z_P)$ (for $Z_P \neq 0$). In Pollard's rho method it is important that P_{i+1} is uniquely determined by P_i. Thus we cannot use a redundant representation but have to work with affine points. For ordinary binary curves $y^2 + xy = x^3 + ax^2 + b$ addition of $P = (x_P, y_P)$ and $Q = (x_Q, y_Q)$ with $x_P \neq x_Q$ is given by

$$(x_R, y_R) = (\lambda^2 + \lambda + a + x_P + x_Q, \lambda(x_R + x_P) + y_P + x_R), \text{ where } \lambda = \frac{y_P + y_Q}{x_P + x_Q}.$$

Each addition needs $1\mathbf{I}$, $2\mathbf{M}$, and $1\mathbf{S}$. Note that one of the multiplications could be combined with the inversion to a division. However, we use a different optimization to reduce the expense of the inversion, the by far most expensive field operation.

5.2   Simultaneous inversion

All machines will run multiple instances in parallel. This makes it possible to reduce the cost of the inversion by computing several inversions simultaneously using a trick due to Montgomery [Mon87]. Montgomery's trick is easiest explained by his approach to simultaneously inverting two elements a and b.

One first computes the product $c = a \cdot b$, then inverts c to $d = c^{-1}$ and obtains $a^{-1} = b \cdot d$ and $b^{-1} = a \cdot d$. The total cost is $1\mathbf{I}$ and $3\mathbf{M}$ instead of $2\mathbf{I}$. By extending this trick to N inputs one can obtain inverses of N elements at the cost of $1\mathbf{I}$ and $3(N-1)\mathbf{M}$.

If N processes are running in parallel on one machine and the implementation uses Montgomery's trick to simultaneously invert all N denominators appearing in the λ's above, the cost per addition decreases to $(1/N)\mathbf{I}$, $(2 + 3(N-1)/N)\mathbf{M}$, and $1\mathbf{S}$; for large N this can be approximated by $5\mathbf{M}$ and $1\mathbf{S}$.

5.3   Inversion

Inversion is by far the most costly of the basic arithmetic operations. Most implementations use one of two algorithms: the Extended Euclidean Algorithm (EEA), published in many papers and books [MvOV96], [ACD+06] and Itoh-Tsujii's method [IT88] which essentially is using Fermat's little theorem.

Let $\mathbf{F}_{2^n}$ be represented in polynomial basis. Each field element f can be regarded as a polynomial over $\mathbf{F}_2$ of degree less than n. The EEA finds elements

u and v such that $fu + Fv = 1$. Then $uf \equiv 1 \bmod F$, $\deg u < n$ and thus u represents the multiplicative inverse of f. The classical EEA performs a full division at each step. In practice for $\mathbf{F}_{2^n} \cong \mathbf{F}_2[X]/F(X)$, implementers often choose a version of the EEA that replaces the divisions with division by X (a right shift of the operand). Although this approach requires more iterations, it is generally faster in practice. This is the approach most commonly seen when elements of $\mathbf{F}_{2^n}$ are represented in polynomial basis but special implementation strategies such as bit slicing are more suited for Itoh-Tsujii.

Although variants of EEA have been developed for normal basis representation [Sun06], the most efficient approach is generally based on Itoh-Tsujii. This algorithm proceeds from the observation that in $\mathbf{F}_{2^n}$, $f^{2^n} = f$, $f^{2^n-1} = 1$, and therefore $f^{2^n-2} = f^{-1}$. Instead of performing divisions as in EEA, this algorithm computes the $2(2^{n-1} - 1)$th power. If f is represented in normal basis, squarings are simply a left shift of the operand. The exponent is fixed throughout the computation, so addition chains can be used to minimize the number of multiplications. For $n = 131$ a minimum-length addition chain to reach 130 is $1, 2, 4, 8, 16, 32, 64, 128, 130$ and the corresponding addition chain on the exponents is $2^1 - 1 = 1, 2^2 - 1, 2^4 - 1, 2^8 - 1, 2^{16} - 1, 2^{32} - 1, 2^{64} - 1, 2^{128} - 1, 2^{130} - 1$.

5.4   Field representation

Typically fields are represented in a polynomial basis using the isomorphism $\mathbf{F}_{2^n} \cong \mathbf{F}_2[z]/F(z)$, where $F(z)$ is an irreducible polynomial of degree n. A basis is given by $\{1, z, z^2, \ldots, z^{n-1}\}$. In this representation addition is done component wise and multiplication is done as polynomial multiplication modulo F. Squaring is implemented as a special case of multiplication; since all mixed terms disappear in characteristic 2 the cost of a squaring is basically that of the reduction modulo F. The Certicom challenges (see Section 2) are given in polynomial-basis representation with F an irreducible trinomial or pentanomial.

An alternative representation of finite fields is to use normal bases. A normal basis is a basis of the form $\{\theta, \theta^2, \theta^{2^2}, \ldots, \theta^{2^{n-1}}\}$ for some $\theta \in \mathbf{F}_{2^n}$. Also in this representation addition is done component wise. Squaring is very easy as it corresponds to a cyclic shift of the coefficient vector: if $c = \sum_{i=0}^n c_i \theta^{2^i}$ then $c^2 = \sum_{i=0}^n c_i \theta^{2^{i+1}} = \sum_{i=0}^n c_{i-1} \theta^{2^i}$, where $c_{-1} = c_n$. Multiplications are significantly more complicated — to express $\theta^{2^i + 2^j}$ in the basis usually a multiplication matrix is given explicitly. If this matrix has particularly few entries then multiplications are faster. The minimal number is $2n - 1$; bases achieving this number are called *optimal normal bases*. For $n = 131$ such a basis exists but for $n = 163$ it does not. Alternatives are to use Gauss periods and redundant representations to represent field elements.

Converting from one basis to the other is done with help of a transition matrix, an $n \times n$ matrix over $\mathbf{F}_2$.

5.5   Cost of one step

In the following sections we will consider implementations on various platforms in different representations — in particular looking at polynomial and normal basis representations. When using distinguished points within the random walk it is important that the walk is defined with respect to a *fixed* field representation. So, if different platforms decide to use different representations it is important to change between bases to find the next step.

   The following sections collect the raw data for the cost of one step, in Section 6 we go into details of how the attack against ECC2K-130 is implemented and give justification.

   For the Koblitz curves when using method 1, each step takes 1 elliptic curve addition, $(n-1)\mathbf{S}$ (to find the lexicographically smallest representative), and $1\mathbf{S}$ to a variable power of the y-coordinate. In particular if $x(P)^{2^m}$ gave the unique representative, one needs to compute $y(P)^{2^m}$. Note that the intermediate powers of $y(P)$ are not needed and special routines can be implemented. We report these figures as m-squarings, costing $\mathbf{mS}$. We do not count the costs for updating the counters a_i and b_i.

   When using method 2 each step takes 1 elliptic curve addition and 2 $\mathbf{mS}$. If the computations are done in polynomial basis, then also the cost for conversion to normal basis need to be considered. If Harley's speedup is used, then the m in the m-squarings is significantly restricted.

6   Fine-tuning of the attack for Certicom ECC2K-130

In this section, we describe the concrete approach we take to attack the DLP on ECC2K-130 defined in Section 2.

6.1   Choice of step function

Of course we use the Frobenius endomorphism and define the walk on classes under Frobenius and negation. Of the two methods described in Section 4 we prefer the second. Advantages are that it can be applied in polynomial basis as well as in normal basis, that it automatically avoids short, fruitless cycles and thus does not require special routines, that there is no need to store pre-computed points, and that it avoids computing the unique representative in the step function (computing the Hamming weight is faster than 130$\mathbf{S}$). If the main computation is done in polynomial-basis representation, a conversion to normal basis is required.

   We analyzed the orders of $(1 + \sigma^j)$ modulo the group order for all small values of j. For $j \geq 3$ no small orders appear. To get sufficient randomness and to have an easily computable step function we compute the Hamming weight of $x(P)$, divide it by 2, reduce the result modulo 8 and add 3. So the updates are $(1 + \sigma^j)$ for $j \in \{3, 4, \ldots, 10\}$. For this set we additionally checked that there does not exist any linear relation with small coefficients between the discrete

logarithms of $(1 + \sigma^j)$ modulo ℓ. The shortest vector in the lattice spanned by the logarithms has four-digit coefficients. This means that fruitless collisions are highly unlikely.

6.2   Heuristic analysis of non-randomness

Consider an adding walk on ℓ group elements that maps P to $P + R_0$ with probability p_0, $P + R_1$ with probability p_1, and so on through $P + R_{r-1}$ with probability p_{r-1}, where $R_0, R_1, \ldots, R_{r-1}$ are distinct group elements and $p_0 + p_1 + \cdots + p_{r-1} = 1$.

If Q is a group element, and P, P' are two independent uniform random group elements, then the probability that P, P' both map to Q without having $P = P'$ is $(1 - p_0^2 - p_1^2 - \cdots - p_{r-1}^2)/\ell^2$. Indeed, if $P = Q - R_i$ and $P' = Q - R_j$, with $i \neq j$, then P maps to Q with probability p_i and P' maps to Q with probability p_j; there is chance $1/\ell^2$ that $P = Q - R_i$ and $P' = Q - R_j$ in the first place; overall the probability is $\sum_{i \neq j} p_i p_j / \ell^2 = (\sum_{i,j} p_i p_j - \sum_j p_j^2)/\ell^2 = (1 - \sum_j p_j^2)/\ell^2$. Adding over the ℓ choices of Q one sees that the probability of an immediate collision from P, P' is at least $(1 - \sum_j p_j^2)/\ell$.

In the context of Pollard's rho algorithm (or its parallelized version), after a total of T iterations, there are $T(T - 1)/2$ pairs of iteration outputs. The inputs are not uniform random group elements, and the pairs are not independent, but one might nevertheless guess that the overall success probability is approximately $1 - (1 - (1 - \sum_j p_j^2)/\ell)^{T(T-1)/2}$, and that the average number of iterations before success is approximately $\sqrt{\pi \ell / (2(1 - \sum_j p_j^2))}$. This is a special case of the variance heuristic introduced by Brent and Pollard in [BP81].

For example, if $p_0 = p_1 = \cdots = p_{r-1} = 1/r$, then this heuristic states that ℓ is effectively divided by $1 - 1/r$, increasing the number of iterations by a factor of $1/\sqrt{1 - 1/r} \approx 1 + 1/(2r)$, as discussed by Teske [Tes01].

The same heuristic applies to a multiplicative walk that maps P to $s_j P$ with probability p_j: the number of iterations is multiplied by $1/\sqrt{1 - \sum_j p_j^2}$. In particular, for the ECC2K-130 challenge, the Hamming weight of $x(P)$ is congruent to $0, 2, 4, 6, 8, 10, 12, 14$ modulo 16 with respective probabilities approximately

$$0.1443, 0.1359, 0.1212, 0.1086, 0.1057, 0.1141, 0.1288, 0.1414,$$

so our walk multiplies the number of iterations by approximately 1.069993. Note that any walk determined by the Hamming weight will multiply the number of iterations by at least $1/\sqrt{1 - \sum_j \binom{131}{2j}^2 / 2^{260}} \approx 1.053211$.

6.3   Choice of distinguished points

In total about $2^{60.9}$ group operations are needed to break the discrete logarithm problem. If we choose Hamming weight 28 for distinguished points then there will be an average length of $2^{35.4}$ steps before hitting a distinguished point,

since $(\binom{131}{28} + \binom{131}{26} + \cdots)/2^{130}$ is approximately $2^{-35.4}$, and an expected number of $2^{25.5}$ distinguished points. Note that for this curve $a = 0$ and thus each x-coordinate has trace 0 and so the Hamming weight is even for any point. If we instead choose Hamming weight 32 for distinguished points then there will be an average length of $2^{28.4}$ steps before hitting a distinguished point and an expected number of $2^{32.5}$ distinguished points.

6.4   Implementation details

Most computations will not lead to a collision. Our implementation does not compute the intermediate scalars a_i and b_i nor does it store a list of how often each of the exponents j appeared. Instead the starting point of each walk is computed deterministically from a salt S. When a distinguished point is found, the salt together with the distinguished point is reported to the central server.

When distinguished points are noticed, $x(P)$ is given in normal basis representation, so it makes sense to keep them in normal basis. To search for collisions it is necessary to have a unique representative per class. We choose the lexicographically smallest value of $x(P), x(P)^2, \ldots, x(P)^{2^{130}}$. In normal basis representation this is easily done by inspecting all cyclic shifts of $x(P)$. To save bandwidth a 64-bit hash of this unique representative is reported to the server along with the original 64-bit seed.

If the server detects a collision on the 64-bit hash, it recovers the two starting points from the salt values and follows the random walk from the initial points, this time keeping track of how often each of the powers j appears. Like in the initial computation the distinguished point is noticed by a small Hamming weight of the normal basis representation of the x-coordinate. If the x-coordinates coincide up to cyclic shifts, i.e. the partial collision gave rise to a complete one, the unique representative per class is computed. Note that this time also the y-coordinate needs to be transformed to normal basis to obtain the correct result.

Finally the equivalence of σ and $s \bmod \ell$ is used to compute the scalars on both sides and thereby (eventually) the $\mathrm{DLP}_P(Q)$.

It is possible for a 64-bit hash collision to occur by accident, rather than from a distinguished-point collision. We could increase the 64-bit hash to 96 bits or 128 bits to eliminate these accidents. However, a larger hash costs bandwidth and server storage, and the benefit is small. Even with as many as 2^{32} distinguished points, accidental 64-bit collisions are unlikely to occur more than a few times, and disposing of the accidents has negligible cost.

We plan to use several servers storing disjoint lists of distinguished points: e.g., server i out of 8 receives the distinguished points where the first 3 hash bits are equal to i in binary. This initial routing means that each server then has to handle only 1/8 of the total volume of distinguished points.

7   FPGA implementations

The attacks presented in this section are developed for the latest version of CO-PACOBANA [KPP+06], which is a tightly integrated, reconfigurable hardware cluster.

The 2009 version of COPACOBANA offers 128 Xilinx Spartan-3 XC3S5000-4FG676 FPGAs, laid out on 16 plug-in modules each hosting 8 chips. Each chip is configured with 32 MB of dedicated off-chip local RAM. Serial data lines connect the FPGAs as a systolic array on the backplane, passing data packets from one device to the next in round robin fashion before they finally reach their destination. Up to two separate controller units interface the systolic array (via PCIe) to the mainboard of a low-profile PC that is integrated within the same case as COPACOBANA. In addition to data routing, the PC can perform post-processing before it stores or distributes the results to other nodes.

This section presents preliminary results comparing two choices for the underlying field arithmetic on COPACOBANA. The first approach performs arithmetic operations on elements represented in polynomial basis, converting to normal basis as needed, while the second operates directly on elements represented in normal basis.

7.1   Polynomial basis implementation

The cycle counts and delay are based on the results of implementations on FPGA (Xilinx XC3S5000-4FG676). For multiplication, digit-serial multiplier is implemented. The choice of digit-size is based on a preliminary exploration of the trade-off between speed and area. Here we choose digit-size $d = 22$ and $d = 24$ for $\mathbf{F}_{2^{131}}$ and $\mathbf{F}_{2^{163}}$, respectively.

For inversion, we used the Itoh-Tsujii algorithm. Although EEA runs faster than Itoh-Tsujii, it requires its own data path, adding extra cost in area. Using Montgomery's trick for batch inversion lowers the amortized cost to $(3-1/N)\mathbf{M}+(1/N)\mathbf{I}$ per inversion. The selection of $N = 64$ is a trade-off between performance and area. One inversion in $\mathbf{F}_{2^{131}}$ takes 212 cycles, and one multiplication takes 8 cycles. Choosing $N = 64$, each inversion on average takes 28 cycles, and the whole design takes 8 out of 104 BRAMs on the target FPGA. If we increase N to 128, the cost of one inversion drops to 26 cycles. However, the whole design requires 16 BRAMs. Since the current design uses around %11 of the LUTs of the FPGA, we can put 8~9 copies of current design onto this FPGA if we do not use more than %11 BRAMs for each.

Tab. 1 shows the cycle counts of each field operation. The cost of memory access is included.

In order to check the Hamming weight of x-coordinate, we convert the x-coordinate to normal basis in each iteration. The basis conversion and population-count operations are performed in parallel and therefore do not add extra delay to the loop.

	additions	squarings	m-squarings	multiplications	inversions	batch-inv. ($N = 64$)
$\mathbf{F}_{2^{131}}$	2	2	m+1	8	212	28
$\mathbf{F}_{2^{163}}$	2	2	m+1	9	251	31

Table 1. Cycle counts for field operations in polynomial basis on XC3S5000-4FG676

The design is synthesized with Xilinx ISE 11.1. On Xilinx XC3S5000-4fg676 FPGA, our current design for $\mathbf{F}_{2^{131}}$ and $\mathbf{F}_{2^{163}}$ can reach a maximum frequency of 74.6 MHz and 74 MHz, respectively. Table 2 shows the delay of one iteration.

	ECC2K-130		ECC2-131	ECC2-163
	Method 1	Method 2		
	$1\mathbf{I} + 2\mathbf{M} + 131\mathbf{S} + 1\mathbf{mS}$	$1\mathbf{I} + 2\mathbf{M} + 1\mathbf{S} + 2\mathbf{mS}$	$1\mathbf{I} + 2\mathbf{M} + 1\mathbf{S}$	$1\mathbf{I} + 2\mathbf{M} + 1\mathbf{S}$
Cycles	371	71	38	51
Delay (ns)	4,971	951	509	714

Table 2. Cost of one iteration in polynomial basis on XC3S5000-4FG676

The current design for ECC2K-130 uses 3,656 slices, including 1,468 slices for multiplier, 75 slices for square, 1,206 slices for base conversion and 117 slices for Hamming Weight counting. Since a Xilinx XC3S5000 FPGA has 33,280 slices, taking input/output circuits into account, we estimate 9 copies of the polynomial-basis design can fit in one FPGA. Considering 2^{35} iterations are required on average to generate one distinguished point, each copy generates 2.6 distinguished points per day. A single chip can then be expected to yield 23.4 distinguished points per day.

The current design for ECC2-131 uses 2,206 slices. Note that circuits to search for the *smallest* $x(P)$ is not included. We estimate that 12 copies (limited by BRAM) can fit in one FPGA.

The current design for ECC2K-163 uses 4,446 slices, including 2,030 slices for multiplier, 94 slices for square and 1,209 slices for base conversion and 217 slices for Hamming Weight counting. We estimate that 7 copies can fit in one FPGA.

The current design for ECC2-163 uses 3,242 slices. Note that circuits to search for the *smallest* $x(P)$ is not included. We estimate that 9 copies can fit in one FPGA.

For ECC2-131, it is the number of BRAM that stops us putting more copies of ECC engine. We believe that the efficiency of BRAMs usage can be further improved, and more copies can be instantiated on one FPGA.

7.2   Normal basis implementation

These estimates are based on an initial implementation of a bit-serial normal-basis multiplier. At the conclusion of this section, we provide an estimate for the

digit-serial version currently under development. The bit-serial design computes a single bit of the product in each clock cycle. Because of this relatively slow performance, it consumes very little area. For $\mathbf{F}_{2^{131}}$, the multiplier takes 466 slices of the chip's available 66,560, or less than 1%, while $\mathbf{F}_{2^{163}}$ requires 679 slices, or around 1%.

	additions	squarings	m-squarings	multiplications	inversions	batch-inversions
$\mathbf{F}_{2^{131}}$	1	1	1	131	1065	
$\mathbf{F}_{2^{163}}$	1	1	1	163	1629	

Table 3. Cycle counts for field operations in normal basis on Xilinx XC3S5000-5FG1156

An implementation of the full Rho step would instantiate at least one multiplier expressly for the Itoh-Tsujii inversion routine and process several points simultaneously to keep the inversion unit busy. Our implementation results take this approach: each engine consists of one multiplier dedicated to inversion and eight for ordinary multiplication. The result for $\mathbf{F}_{2^{131}}$ is an area requirement of 1,915 slices while achieving a clock rate of 85.898 MHz.

The inversion unit is the bottleneck at 1,065 cycles required. We can use Montgomery's trick to perform many simultaneous inversions. So the design challenge becomes one of keeping the inversion unit busy, spreading the cost of the inverter across as many simultaneous Rho steps as possible.

Suppose we process 32 inversions simultaneously using one inversion unit. This operation introduces $8\mathbf{M}$ cycles of delay. Method 2 requires $1\mathbf{I}+2\mathbf{M}+1\mathbf{S}+1\mathbf{mS}$ to compute one step of the Rho method. Because squarings are free, we must compute two additional multiplications per step. On top of this cost are the $3(N-1) = 157$ multiplications needed for the pre- and post-computation to obtain individual inverses. Although we might be able to spread a particular step across several multipliers, we can safely assume that keeping the inversion unit busy this way requires up to a total of 32 additional multipliers. The chip has embedded storage for up to 1,664 points, far more than required. With this approach, these multipliers would be idle roughly five-eighths of the time; this estimate is meant to be conservative. At a cost of 466 slices each, we can expect an engine to consume a total of 14,912 slices. Instantiating all these multipliers has the advantage that we can complete 32 steps every 1,065 cycles, or one step every 34 cycles. At 85.898 MHz, that equates to 2,526,411 steps per second, or 6 distinguished points per day per engine. As a single chip has 66,360 slices available, four of these engines could be instantiated per chip, yielding 24 distinguished points per day per chip. This figure may underestimate the time required for overhead like memory access.

Mitigating this effect is the fact that the time-area product can surely be improved by modifying the multiplier to use a digit-serial approach as described in [NS06]. This time-area tradeoff processes d bits of the product simultaneously

at a cost of additional area. We are currently implementing this approach; the previous work indicates that this approach can improve the time-area product.

As of this writing, normal-basis results for $\mathbf{F}_{2^{163}}$ are still pending.

7.3   Comparison

Both polynomial and normal-basis implementations offer roughly the same performance today. Because the polynomial-basis implementation is in a more mature state, embodying the entire step of the Rho method, it represents less risk and uncertainty in terms of use in a practical attack. It achieves this performance despite the fact that this particular Certicom challenge would appear to be ideally suited to a normal-basis implementation. As a case in point, the polynomial version must pay the overhead to convert elements back to normal basis at the end of each step to check if a distinguished point has been reached.

As this paper represents work in progress, the normal-basis figures in this section are based on measurements only of the field arithmetic time and area. While the estimates may not fully account for overhead like memory access, they also do not capture the effect of migrating to a digit-serial multiplier. Because multiplication cost dominates the cost of inversion – and therefore the cost of a step of the Rho method, the normal-basis approach may ultimately offer higher performance because in this particular attack. Performance of the polynomial-basis version may also improve in unforeseen ways and it would undoubtedly outperform the normal-basis version in an attack on ECC2-131.

8   Hardware implementations

In this section we present and discuss the results achieved while targeting ASIC platforms. To obtain the estimates presented in this work, we have used the UMC L90 CMOS technology, using the Free Standard Cell library from Faraday Technology Corporation characterized for HS-RVT (high speed regular Vt) process option with 8 Metal layers. For synthesis results we have used design compiler 2008.09 from Synopsys, and for placement and routing we have used SoC Encounter 7.1-usr3 from Cadence Design Systems.

Both synthesis and post-layout analysis use typical corner values, and reasonable assumptions for constraints. The designs are for performance estimate and are not refined for actual production (i.e. they do not contain test structures, a practical I/O subsystem). During synthesis, multiple runs were made with different constraints, and the results with the best area time product have been selected.

8.1   Polynomial basis implementation

For the polynomial basis, the estimates are based on the work presented by Meurice de Dormale et al. in [MdDBQ07] and Bulens et al. in [BMdDQ06] where the authors proposed an implementation based on a pipelined architecture.

Addition The addition of n-bits will always be equal to $2n$-input XOR gates. No separate synthesis has been made for this circuit. In a practical circuit the interconnection between the adder the rest of the circuit would have a significant impact upon the delay and the area of the circuit. The delay for the addition is approximately 75 ps, while the required area is approximately $n \cdot 2.5$ Gate Equivalents (GEs). No post-layout results are given for this circuit as a standalone implementation is not representative.

Squaring Squaring is performed with a parallel squarer. This operator is relatively inexpensive thanks to the use of a sparse irreducible polynomial, a pentanomial, which is hardwired. Each bit of the result is therefore computed using few XOR gates. The detailed results for ASIC implementation are reported in Table 4, where, due to the small size of this component, no post-layout analysis is provided.

	$\mathbf{F}_{2^{131}}$	$\mathbf{F}_{2^{163}}$
	Pre-layout	Pre-layout
Delay (ps) $\sim$	250	250
Frequency (GHz) $\sim$	4.0	4.0
Flip-Flop Number	131	163
Area (mm^2) $\sim$	0.003	0.004
GE $\sim$	960	1200

Table 4. Results for ASIC implementation of Squarer in polynomial basis

m-**Squaring** This operation can be implemented using a single squarer that iteratively computes the m squarings in m clock cycles.

Multiplication In order to perform the modular multiplication, we used a sub-quadratic Karatsuba parallel multiplier. As for squaring, the modular reduction step is easily performed with a few XOR gates for each bit of the result. The modular multiplier has a pipeline depth of 8 clock cycles in both $\mathbf{F}_{2^{131}}$ and $\mathbf{F}_{2^{163}}$ and produces a result at each clock cycle. The detailed results for the modular multiplication are reported in Table 5

	$\mathbf{F}_{2^{131}}$		$\mathbf{F}_{2^{163}}$	
	Pre-layout	Post-layout	Pre-layout	Post-layout
Delay (ps) $\sim$	470	585	500	575
Frequency (GHz) $\sim$	2.1	1.7	2.0	1.7
Flip-Flop Number	4608	4608	5768	5768
Area (mm^2) $\sim$	0.175	0.185	0.227	0.250
GE $\sim$	55000	59000	72500	80000

Table 5. Results for ASIC implementation of Multiplication in polynomial basis

Inversion The inversion is based on Fermat's little theorem with the multiplication chain technique by Itoh and Tsujii. This method is preferred to the extended Euclidean algorithm according to the comparison of both methods performed in the work by Bulens et al. [BMdDQ06]. An inversion requires 130 squarings and 8 multiplications in $\mathbf{F}_{2^{131}}$ and 162 squarings and 9 multiplications in $\mathbf{F}_{2^{163}}$. The inverter uses the parallel multiplier described above and a block of several pipelined consecutive squarers. This block allows to speed up the consecutive squarings required in the inversion using the Itoh-Tsujii technique. It is done by putting several squarers in a serial way, so that every bit of the result is now computed with a larger number of XOR gates, depending on the number of squarings to be performed. Within the inverter, the block of consecutive squarers actually allows to compute several possible numbers of consecutive squarings (the numbers of consecutive squarings specified by the technique of Itoh and Tsujii). The inversion is done by looping over the multiplier and the squarer according to the technique of Itoh and Tsujii. For this purpose, extra shift registers are required. The inverter has a pipeline depth of 16 and achieves an inversion with a mean delay of 10 and 11 clock cycles in $\mathbf{F}_{2^{131}}$ and $\mathbf{F}_{2^{163}}$ respectively.

A lower bound on the area requirement of the inverter can be found by gathering the results for the squarer and the multiplier. This leads to around 60000 GE for $\mathbf{F}_{2^{131}}$ and 81200 for $\mathbf{F}_{2^{163}}$. However, this assumes an iterative use of the squarer. For the parallel pipelined inverter described above, a better estimate can be obtained by approximating the block of consecutive squarers as a series of single squarers. The number of these consecutive squarers is given by the maximum number of consecutive squarings in the technique of Itoh and Tsujii on $\mathbf{F}_{2^{131}}$ and $\mathbf{F}_{2^{163}}$, i.e. 64 in both cases. As a result, the area cost of the block of consecutive squarers should be around 64000 and 76800 GE for $\mathbf{F}_{2^{131}}$ and $\mathbf{F}_{2^{163}}$ respectively, leading to an area cost of 123000 GE and 156800 for the full parallel inverter on $\mathbf{F}_{2^{131}}$ and $\mathbf{F}_{2^{163}}$ respectively.

The inverter has a much higher area cost and lower throughput with respect to the multiplier. From an area-time point of view, it is interesting to combine several inversions using the Montgomery trick instead of replicating several inverters when trying to increase the throughput of inversions. As each combined inversion requires 3 multiplications to be performed, it seems to be always interesting to use the Montgomery trick instead of replicating several inverters. In practice, the gain of using Montgomery's trick can be smaller than expected, as stated in [BMdDQ06]. Simultaneous inversion does not require a specific operator as it can be built upon the multiplier and the inverter.

Conversion A conversion from polynomial to normal basis is required when using method 2 as described in Section 4.2. The detailed results for this operation are reported in Table 6.

	$\mathbf{F}_{2^{131}}$	$\mathbf{F}_{2^{163}}$
	Pre-layout	Pre-layout
Delay $(ps) \sim$	410	460
Frequency $(GHz) \sim$	2.4	2.15
Flip-Flop Number	0	0
Area $(mm^2) \sim$	0.044	0.061
GE $\sim$	13900	19400

Table 6. Results for ASIC implementation of Polynomial to Normal Basis converter

	additions	squarings	m-squarings	multiplications	inversions
$\mathbf{F}_{2^{131}}$	1	1	m	1	10
$\mathbf{F}_{2^{163}}$	1	1	m	1	11

Table 7. Cycle counts for field operations in polynomial basis on ASIC

8.2   Normal basis implementation

Addition For ASIC, the addition is performed in a way similar to the one of polynomial bases.

Squaring In normal basis, the squaring is equivalent to a rotation, thus the impact on the area and delay of this component will be mainly due to the interconnections.

m**-Squaring** This operation can be achieved by an iterative use of a single squarer as for the polynomial basis. However, since a squaring is equivalent to a rotation, one can anticipate the m rotations and perform this operation in one clock cycle.

Multiplication The proposed implementation is based on a bit-serial multiplier which calculates a single bit product every clock cycle. The detailed results for the modular multiplication are reported in Table 8.

	$\mathbf{F}_{2^{131}}$		$\mathbf{F}_{2^{163}}$	
	Pre-layout	Post-layout	Pre-layout	Post-layout
Delay $(ps) \sim$	510	550	485	576
Frequency $(GHz) \sim$	2.0	1.8	2.0	1.75
Flip-Flop Number	402	402	661	611
Area $(mm^2) \sim$	0.015	0.016	0.025	0.027
GE $\sim$	5000	5250	7900	8800

Table 8. Results for ASIC implementation of Field element multiplier in normal basis

Inversion Also in normal bases, the inversion is implemented using Fermat's little theorem, thus the considerations of Section 8.1 hold also in this case. The number of cycle counts for the operations in normal basis on ASIC are shown in Table 9. The area requirement of the inverter in normal basis

should not be significantly higher than the cost of the multiplier since the multiple squarings can be performed with interconnections only. Therefore, it should be close to the lower bound given by the area cost of the multiplier, i.e. 5250 GE for $\mathbf{F}_{2^{131}}$.

	additions	squarings	m-squarings	multiplications	inversions
$\mathbf{F}_{2^{131}}$	1	1	1	131	1178
$\mathbf{F}_{2^{163}}$	1	1	1	163	1629

Table 9. Cycle counts for field operations in normal basis on ASIC

8.3 Cost of step on ECC2K-130

A step in the Pollard rho computation on ECC2K-130 consumes $1\mathbf{I}+2\mathbf{M}+131\mathbf{S}+1\mathbf{mS}$ using method 1. In polynomial basis, this takes 273 cycles on an ASIC while in normal basis it takes 1572 cycles. Using method 2, a step requires $1\mathbf{I}+2\mathbf{M}+1\mathbf{S}+2\mathbf{mS}$ and the additional conversion to normal basis if the computations are done in polynomial basis. In polynomial basis, the step is performed in 274 cycles on an ASIC while in normal basis it is done in 1443 cycles. A larger cycle count for the normal basis is due to the iterative approach of the design of the components in this basis as opposed to the parallel design used for the polynomial basis. These cycles counts do not consider the use of simultaneous inversion since the gain of this method should be assessed once the whole processor is assembled, following [BMdDQ06]. This technique should be employed as much as possible given the high cost of an inversion. Therefore, the cycle counts are likely to be significantly lower in practice. For instance, combining 10 inversions theoretically lowers the cycle count for the step in normal basis by about 50%.

Concerning the area, a lower bound can be determined by gathering the costs of the operators. Note that this bound does not include the cost of storing elements. In polynomial basis, the lower bound on the area of a processor based on the components described above is roughly 125000 GE when using method 1 and 140000 GE for method 2. It is mostly the cost of the inverter, as its multiplier can also be used to perform the two multiplications needed in each step. In normal basis, the same estimate leads to 6000 GE (mainly the cost of the multiplier). Based on these estimates, the processor relying on the normal basis appears to be more efficient from an area-time point of view as it is roughly 6 times slower but 20 times smaller. However, the use of several squarers in parallel should improve the area-time product of the processor relying on the polynomial basis.

8.4 Cost of step on ECC2-131

A step in the Pollard rho computation on ECC2-131 consumes $1\mathbf{I}+2\mathbf{M}+1\mathbf{S}$. In polynomial basis this takes 13 cycles on ASIC while in normal basis it takes

1441 cycles. Again, the iterative approach used in the normal basis causes a higher cycle count for the normal basis operators. The area costs are on the same order as on ECC2K-130. Therefore, the processor based on the polynomial basis appears to be more efficient here since it is 110 faster while being only 20 times larger.

8.5   Cost of step on ECC2-163

A step in the Pollard rho computation on ECC2-163 consumes $1\mathbf{I} + 2\mathbf{M} + 1\mathbf{S}$. In polynomial basis this takes 14 cycles on ASIC while in normal basis it takes 1956 cycles.

The processor based on the polynomial basis has a lower bound on the area cost around 160000 GE (mainly the cost of the inverter). It is 140 times faster than the one based on the normal basis. For this reason, it is expected to be more area-time efficient, as on ECC2-131.

8.6   Detailed cost of the full attack on ECC2K-130

With the cost of individual arithmetic blocks given above, we can now attempt a first order estimation of cost and performance of an ASIC that could be used for the ECC2K-130 challenge. We will consider using a standard 16mm2 die in the 90nm CMOS technology using a multi-project wafer (MPW) production in prototype quantities. The cost of producing and packaging 50-250 of such ASICs is estimated to be less than 60 000 EUR.

The performance of the subcomponents described in the preceding sections were all post-layout figures that include interconnection delays, clock distribution overhead and all required registers. We estimate that the overall clock rate will be around 1.5 GHz when all the components are combined into one system. Each chip would require a PLL for to distribute the internal clock. In this estimation we will again leave a generous margin in the timing and will assume that the system clock is 1.25 GHz.

When using the specific standard cell library the 16mm2, 90nm CMOS die has a net core area of 12mm2, which could support approximately 3.000.000 gates with generous overhead for power routing and placement. Reserving 1.000.000 gates for PLL, I/O interface and a shared point inspection unit, we will consider that only 2.000.000 gates will be available for point calculation units. A single chip could thus support 400 cores in parallel. Considering that each core requires 1572 clock cycles per iteration (section 7.3), such an ASIC would be able to calculate approximately 320 Miterations/s. The estimation of the complete attack able to break ECC2K-130 in one year would require approximately 69 000 Miterations/s. Even our overly pessimistic estimation shows that this performance can be achieved by a modest collection of around 220 dedicated ASICs.

9   AMD64 implementations

This section describes our software implementation for general-purpose CPUs supporting the amd64 (also known as "x86-64") instruction set. This implementation is tuned for Intel's popular Core 2 series of CPUs but also performs reasonably well on other recent CPUs, such as the AMD Phenom.

9.1   Bitslicing

New speed records for elliptic-curve cryptography on the Core 2 were recently announced in a Crypto 2009 paper [Ber09a]. The new speed records combine a fast complete addition law for binary Edwards curves, fast bitsliced multiplication for arithmetic in $\mathbf{F}_{2^n}$, and the Core 2's fast instructions for arithmetic on 128-bit vectors. Our amd64 implementation combines the bitsliced multiplication techniques from [Ber09a] with several additional techniques for bitsliced computation. (Binary Edwards curves do not appear to save time in this context; the implementation uses standard affine coordinates for Weierstrass curves.)

Bitslicing a data structure is a simple matter of transposition. Our implementation represents 128 elliptic-curve points $(x_0, y_0), (x_1, y_1), \ldots, (x_{127}, y_{127})$, with $x_i, y_i \in \mathbf{F}_{2^n}$, as $2n$ vectors $X_0, X_1, \ldots, X_{n-1}, Y_0, Y_1, \ldots, Y_{n-1}$, where the jth bits of X_i and Y_i are the ith bits of x_j and y_j respectively.

"Logical" vector operations act on bitsliced inputs as 128-way SIMD instructions. For example, a vector XOR carries out xors in parallel on 128 pairs of bits. Multiplication in $\mathbf{F}_{2^n}$ can be decomposed into bit operations, a series of bit XORs and bit ANDs; one can carry out 128 multiplications on 128 pairs of bitsliced inputs in parallel by performing the same series of vector XORs and vector ANDs. XOR and AND are not the only operations available, but other operations do not seem helpful for multiplication, which takes most of the time in this implementation.

Similar comments apply to higher-level computations, such as elliptic-curve arithmetic over $\mathbf{F}_{2^n}$. There is an obvious analogy between designing bitsliced software and designing ASICs, but one should not push the analogy too far: there are fundamental differences in gate costs, communication costs, etc.

Many common software-implementation techniques for $\mathbf{F}_{2^n}$ arithmetic, such as precomputed multiplication tables, perform quite badly when expressed as bit operations. However, bitslicing allows free shifts, masks, etc., and fast bitsliced algorithms for binary-field arithmetic outperform all known non-bitsliced algorithms.

9.2   Results

Tables 10 and 11 show measurements of the number of cycles per input used for various computations. These measurements are averages across billions of steps.

Elliptic-curve addition uses $\mathbf{1I} + \mathbf{2M} + \mathbf{1S}$, and computing the input to the addition uses $\mathbf{20S}$. (A non-bitsliced algorithm would use only $\mathbf{13S}$ on average, but

	addition	squaring	multiplication	inversion	normal	step
$\mathbf{F}_{2^{131}}$	3.5625	2.6406	85.32	1089.4	103.84	694
$\mathbf{F}_{2^{163}}$	4.0625	2.9141	140.35	1757.18	157.58	1059

Table 10. Cycle counts per input for bitsliced field operations in polynomial basis on a 3000MHz Core 2 Q6850 6fb

	addition	squaring	multiplication	inversion	normal	step
$\mathbf{F}_{2^{131}}$	4.4141	3.8516	101.40	1509.9	59.063	778
$\mathbf{F}_{2^{163}}$	4.9688	4.5859	170.98	2460.9	129.180	1249

Table 11. Cycle counts per input for bitsliced field operations in polynomial basis on a 2200MHz Phenom 9550 100f23

squarings are not the main operation in this implementation.) The implementation batches $48\mathbf{I}$ into $1\mathbf{I} + 141\mathbf{M}$, and then computes $1\mathbf{I}$ as $8\mathbf{M} + 130\mathbf{S}$ (in the case of ECC2K-130), so on average each inversion costs $3.10417\mathbf{M} + 2.70833\mathbf{S}$. The total cost of field arithmetic in a step is therefore $5.10417\mathbf{M} + 23.70833\mathbf{S}$. The "step" cycle count shown above includes more than field arithmetic:

- About 63% of the time (on a Core 2) is spent on multiplications.
- About 15% of the time is spent on conversion to normal-basis representation. This computation uses the algorithm described in [Ber09b].
- About 9% of the time is spent on squarings.
- About 7% of the time is spent on additions.
- About 3% of the time is spent on weight calculation. This calculation combines standard full-adder circuits in an obvious way, adding (for example) 15 bits by first adding 7 bits, then adding 7 more bits, then adding the two sums to the remaining bit.
- The remaining 3% of the time is spent on miscellaneous overhead.

The 48 inversions are actually 48 bitsliced inversions of $48 \cdot 128$ field elements, each containing n bits. The implementation handles $48 \cdot 128$ points (x, y) in parallel. Each x-coordinate (in batches of 128) is converted to normal-basis representation, compressed to a Hamming weight, checked for being distinguished, and then further compressed to three bits that determine the point (x', y') that will be added to (x, y). The implementation computes each x' by repeated squaring, stores $x' + x$ along with (x, y), and inverts $x' + x$. The total active memory for all $x, y, x' + x, 1/(x' + x)$ is $4 \cdot 48 \cdot 128$ field elements, together occupying $3072n$ bytes: i.e., 402432 bytes for $n = 131$, or 500736 bytes for $n = 163$. Subsequent elliptic-curve operations use only a few extra field elements.

10   Cell implementations

Jointly developed by Sony, Toshiba and IBM, the Cell Broadband Engine (Cell) architecture [Hof05] is equipped with one dual-threaded, 64-bit in-order Power

Processing Element (PPE), which can offload work to the eight Synergistic Processing Elements (SPEs) [TCC+05]. Each SPE consists of a Synergistic Processing Unit (SPU), 256 kilobytes of private memory called Local Store (LS), a Memory Flow Controller, and a register file containing 128 registers of 128 bits each. The SPUs are the target of our Cell implementation and allow 128-bit wide single instruction, multiple data (SIMD) operations. The SPUs are asymmetric processors, having two pipelines (denoted by the odd and the even pipeline) which are designed to execute two disjoint sets of instructions. Hence, in the ideal case, two instructions can be dispatched per cycle.

All performance measurements for the Cell stated in this section are obtained by running on a single SPE on a PlayStation 3 (PS3) video game console on which the programmer has access to six SPEs.

Like the amd64 architecture, the SPU supports bit-logical operations on 128-bit registers. Hence, a bitsliced implementation — similar to the one presented in Section 9 — seems to be a good approach. However, for two reasons it is much harder to achieve good performance with the same techniques on the SPU:

The first reason is the restricted local storage size of only 256 KB. As bitsliced implementations work on 128 inputs in parallel, they need much more memory for intermediate values than a non-bitsliced implementation. Even if the code and intermediate results fit into 256 KB, the batch size for Montgomery inversions has to be smaller yielding a higher number of costly inversions per iteration. The second reason is that all instructions are executed in order; a fast implementation requires loop unrolling in several functions increasing the code size and limiting the available storage for batching even further.

We decided to implement both a bitsliced version and a non-bitsliced version to compare which approach gives better results for the SPE. Both implementations required hand-optimizing the code on the assembly level, the main focus is on the ECC2K-130 challenge.

10.1   Non-bitsliced implementation

We decided to represent 131-bit polynomials using two 128-bit vectors. Let $A, B \in \mathbf{F}_{2^{131}}$ in polynomial basis. In order to use 128-bit look-up tables and to get 16-bit aligned intermediate results the multiplication is broken into parts as follows

$$A = A_l + A_h \cdot z^{128} = \widetilde{A}_l + \widetilde{A}_h \cdot z^{121}$$
$$B = B_l + B_h \cdot z^{128} = \widetilde{B}_l + \widetilde{B}_h \cdot z^{15}$$
$$C = A \cdot B = \widetilde{A}_l \cdot B_l + \widetilde{A}_l \cdot B_h \cdot z^{128} + \widetilde{A}_h \cdot \widetilde{B}_l \cdot z^{121} + \widetilde{A}_h \cdot \widetilde{B}_h \cdot z^{136}$$

For the first two multiplications a four bit lookup table and for the third and fourth a two bit lookup table are used. The squaring is implemented by inserting a 0 bit between consecutive bits of the binary representation. In order to hide latencies two steps are interleaved aiming at filling both pipelines in order to reduce the total number of required cycles. The m-squarings are implemented using look-up tables for $3 \le m \le 10$ and take for any such value of m a constant

number of cycles. The inversion is implemented using a sequence of squarings, m-squarings and multiplications.

The optimal number of concurrent walks is as large as possible, i.e. such that the executable and all the required memory fit in the LS. In practice 256 walks are processed in parallel.

	addition	squaring	m-squaring	multiplication	inversion	normal	step
$\mathbf{F}_{2^{131}}$	1 - 2	38	96	149	8000	96	1157

Table 12. Cycle counts per input for non-bitsliced field operations in polynomial basis on one SPE of a 3192 MHz Cell Broadband Engine, rev. 5.1

Cost of step on ECC2K-130 A step in the Pollard rho computation on ECC2K-130 consumes $\frac{1}{256}\mathbf{I} + 5\mathbf{M} + 1\mathbf{S} + 2m\mathbf{S}$ plus the conversion from polynomial to normal basis when using method 2 as described in Section 4.2. The required number of cycles for one iteration on the curve ECC2K-130 are stated in Table 12. Addition is done by two XOR instructions, which go in the even pipeline, and requires at most two and at least one instruction if interleaved with two odd instructions. There are 55 miscellaneous cycles which include the additions, the calculation of the weight, the test if a point is distinguished and various overhead. The cycle counts stated in Table 12 are obtained by "counting" the required number of cycles of our assembly code with the help of the SPU timing tool: a static timing analysis tool available for the Cell.

10.2   Bitsliced implementation

The bitsliced implementation is based on the C++-code for the amd64 architecture. In a first step we ported the code to C, to reduce the size of the resulting binary. For the ECC2K-130 we then implemented bitsliced versions of multiplication, reduction, squaring, addition and conditional move (cmov) in assembly to accelerate the computations.

The maximal batch size that we can use for the ECC2K-130 challenge is 14. Timings for the implementation are given in Table 13, all timings include costs for function calls, they ignore costs for reading the input, which is negligible for long computations until a distinguished point has been found. The measurements are averages across billions of steps measured at runtime.

As for the amd64 implementation, elliptic-curve addition uses $1\mathbf{I} + 2\mathbf{M} + 1\mathbf{S}$, and computing the input to the addition uses $20\mathbf{S}$. The implementation batches $13\mathbf{I}$ into $1\mathbf{I} + 36\mathbf{M}$, and then computes $1\mathbf{I}$ as $8\mathbf{M} + 130\mathbf{S}$ so on average each inversion costs $3.3846\mathbf{M} + 10\mathbf{S}$. The total cost of field arithmetic in a step is therefore $5.3846\mathbf{M} + 31\mathbf{S}$. The "step" cycle count shown above includes more than field arithmetic:

	addition	cmov	squaring	multiplication	inversion	normal	step
$\mathbf{F}_{2^{131}}$	5.8438	6.3125	4.5859	127.5938	1845.3125	30.7734	1046.8359

Table 13. Cycle counts per input for bitsliced field operations in polynomial basis on one SPE of a 3192 MHz Cell Broadband Engine, rev. 5.1

- About 60% of the time is spent on multiplications.
- About 3% of the time is spent on conversion to normal-basis representation.
- About 12% of the time is spent on squarings.
- About 3% of the time is spent on additions.
- About 3% of the time is spent on conditional moves.
- About 11% of the time is spent on weight calculation.
- The remaining 8% of the time is spent on miscellaneous overhead.

For algorithmic details see also Section 9.

11   Complete implementation of the attack

Eventually all platforms described so far will be used to attack ECC2K-130. As a proof of concept and as infrastructure for our optimized implementations we built `ref-ntl`, a C++ reference implementation of an ECC2K discrete-logarithm attack using Shoup's NTL for field arithmetic. The implementation has several components:

- Descriptions of several different ECC2K challenges that the user can target. Similarly to the data in Section 2 each description consists of an irreducible polynomial F, curve parameters a, b, curve points P, Q in hexadecimal, the order ℓ of P, the root s of $T^2 + (-1)^a T + 2$ modulo ℓ that corresponds to the Frobenius endomorphism (so that $\sigma(P) = [s]P$), a choice of normal-basis generator, and a choice of weight defining distinguished points.
- A `setup` program that converts a series of 64-bit seeds $t_1, t_2, \ldots$ into a series of curve points $A(t_1)P \oplus Q, A(t_2)P \oplus Q, \ldots$. The function A uses AES to expand each seed t_j into a bit-string $(c_{j,127}, c_{j,126}, \ldots, c_{j,1}, c_{j,0})$ of length 128 and then interprets it as a Frobenius expansion to compute starting point $Q \oplus \sum_{i=0}^{127} c_{j,i}\sigma^i(P)$.
- An `iterate` program that given an elliptic curve point iterates the step function until a distinguished point is found and then reports it to a server. This computation is the real bottleneck in the implementation; the task of the optimized implementations in Sections 7–10 is to perform the same computation as quickly as possible on various platforms.
- A short script that normalizes each distinguished point and sorts the normalized distinguished points to find collisions.
- A verbose variant of the `iterate` program that, starting from two colliding seeds, recomputes the corresponding distinguished points while keeping track of the iteration steps. This recomputation takes negligible time and removes

the need for the optimized implementations to keep track of the iteration steps.

- Final programs `finish` and `verify` that express each of the colliding normalized distinguished points as linear combinations of P and Q and that print the discrete logarithm of Q base P.

As an end-to-end test of the implementation we solved a randomly generated challenge over $\mathbf{F}_{2^{41}}$, using about one second of computation on one core of a 2.4GHz Core 2 Quad. We checked the result using the Magma computer-algebra system. We then solved ECC2K-95, as described in Section 1.

References

[ACD+06] Roberto Avanzi, Henri Cohen, Christophe Doche, Gerhard Frey, Tanja Lange, Kim Nguyen, and Frederik Vercauteren. *Handbook of Elliptic and Hyperelliptic Curve Cryptography*. CRC Press, 2006.

[Ber09a] Daniel J. Bernstein. Batch binary Edwards. In *Crypto 2009*, volume 5677 of *LNCS*, pages 317–336, 2009.

[Ber09b] Daniel J. Bernstein. Optimizing linear maps modulo 2, 2009. `http://cr.yp.to/papers.html#linearmod2`.

[BMdDQ06] Philippe Bulens, Guerric Meurice de Dormale, and Jean-Jacques Quisquater. Hardware for Collision Search on Elliptic Curve over $\mathrm{GF}(2^m)$. In *Proceedings of SHARCS'06*, 2006. `http://www.hyperelliptic.org/tanja/SHARCS/talks06/bulens.pdf`.

[BP81] Richard P. Brent and John M. Pollard. Factorization of the eighth Fermat number. *Mathematics of Computation*, 36:627–630, 1981.

[Cer97a] Certicom. Certicom ECC Challenge. `http://www.certicom.com/images/pdfs/cert_ecc_challenge.pdf`, 1997.

[Cer97b] Certicom. ECC Curves List. `http://www.certicom.com/index.php/curves-list`, 1997.

[GLV00] Robert P. Gallant, Robert J. Lambert, and Scott A. Vanstone. Improving the parallelized Pollard lambda search on anomalous binary curves. *Mathematics of Computation*, 69(232):1699–1705, 2000.

[Har] Robert Harley. Elliptic curve discrete logarithms project. `http://pauillac.inria.fr/~harley/ecdl/`.

[Har60] Bernard Harris. Probability distributions related to random mappings. *The Annals of Mathematical Statistics*, 31:1045–1062, 1960.

[Hof05] H. Peter Hofstee. Power efficient processor architecture and the Cell processor. In *HPCA 2005*, pages 258–262. IEEE Computer Society, 2005.

[IT88] Toshiya Itoh and Shigeo Tsujii. A Fast Algorithm for Computing Multiplicative Inverses in $GF(2^m)$ Using Normal Bases. *Inf. Comput.*, 78(3):171–177, 1988.

[KPP+06] S. Kumar, C. Paar, J. Pelzl, G. Pfeiffer, and M. Schimmler. Breaking ciphers with COPACOBANA-a cost-optimized parallel code breaker. *Lecture Notes in Computer Science*, 4249:101, 2006.

[MdDBQ07] Guerric Meurice de Dormale, Philippe Bulens, and Jean-Jacques Quisquater. Collision Search for Elliptic Curve Discrete Logarithm over $\mathrm{GF}(2^m)$ with FPGA. In *Workshop on Cryptographic Hardware and Embedded Systems (CHES 2007)*, pages 378–393. Springer, 2007.

[Mon87]   Peter L. Montgomery. Speeding the Pollard and elliptic curve methods of factorization. *Mathematics of Computation*, 48:243–264, 1987.

[MvOV96]   A.J. Menezes, P.C. van Oorschot, and S.A. Vanstone. *Handbook of Applied Cryptography*. CRC Press, 1996.

[NS06]   M. Novotnỳ and J. Schmidt. Two Architectures of a General Digit-Serial Normal Basis Multiplier. In *Proceedings of 9th Euromicro Conference on Digital System Design*, pages 550–553, 2006.

[Pol78]   John M. Pollard. Monte Carlo methods for index computation (mod p). *Mathematics of Computation*, 32:918–924, 1978.

[Sun06]   Berk Sunar. A Euclidean algorithm for normal bases. *Acta Applicandae Mathematicae*, 93:57–74, 2006.

[TCC$^+$05] Osamu Takahashi, Russ Cook, Scott Cottier, Sang H. Dhong, Brian Flachs, Koji Hirairi, Atsushi Kawasumi, Hiroaki Murakami, Hiromi Noro, Hwa-Joon Oh, Shoji Onish, Juergen Pille, and Joel Silberman. The circuit design of the synergistic processor element of a Cell processor. In *ICCAD 2005*, pages 111–117. IEEE Computer Society, 2005.

[Tes01]   Edlyn Teske. On random walks for Pollard's rho method. *Mathematics of Computation*, 70(234):809–825, 2001.

[vOW99]   Paul C. van Oorschot and Michael J. Wiener. Parallel collision search with cryptanalytic applications. *Journal of Cryptology*, 12(1):1–28, 1999.

[WZ98]   Michael J. Wiener and Robert J. Zuccherato. Faster attacks on elliptic curve cryptosystems. In *Selected Areas in Cryptography*, volume 1556 of *LNCS*, pages 190–200, 1998.